



**University of
Zurich^{UZH}**

**Zurich Open Repository and
Archive**

University of Zurich
University Library
Strickhofstrasse 39
CH-8057 Zurich
www.zora.uzh.ch

Year: 2017

Neurodegeneration in the spinal ventral horn prior to motor impairment in cervical spondylotic myelopathy

Grabher, Patrick ; Mohammadi, Siawoosh ; David, Gergely ; Freund, Patrick

Abstract: Remote grey matter pathology has been suggested rostral to the compression site in cervical spondylotic myelopathy (CSM). We used computational neuroimaging to assess in-vivo the extent and functional relevance of neurodegeneration in ventral and dorsal horns above the site of compression in the cervical cord of CSM patients. Twenty patients with CSM and eighteen healthy subjects underwent a high-resolution structural and diffusion MRI protocol at vertebra C2/C3. Patients received comprehensive clinical assessments. T2*-weighted data were used to segment the cross-sectional area of the grey matter into the ventral and dorsal horns. Within the ventral and dorsal horns mean diffusivity (MD) and fractional anisotropy (FA) derived from diffusion tensor imaging data determined the underlying microstructural integrity. Finally, the relationships between neurodegeneration occurring in the grey and white matter and clinical impairment were investigated. Patients suffered from mild to moderate CSM with mainly sensory impairment. The cross-sectional area of the ventral horns was not reduced ($p=0.863$) when compared to controls, but MD was increased ($p=0.045$). Greater increases in MD within the ventral horn were associated with white matter diffusivity changes (increased MD: $p=0.013$; decreased FA: $p=0.028$) within the lateral corticospinal tract. In contrast, dorsal horn cross-sectional area was reduced by 16.0% ($p<0.001$) without alterations in diffusivity indices when compared to controls. No associations between neurodegeneration and clinical impairment were evident. Grey matter atrophy and microstructural changes are evident remote to the compression site in CSM patients. Prior to marked motor impairment, pathophysiological changes in the ventral horns (e.g. motoneurons) related to white matter changes within the corticospinal tract. Thus, neuroimaging biomarkers of cord grey matter integrity reveal focal neurodegeneration prior to marked clinical impairment and thus could serve as predictors of ensuing impairment in CSM patients.

DOI: <https://doi.org/10.1089/neu.2017.4980>

Posted at the Zurich Open Repository and Archive, University of Zurich

ZORA URL: <https://doi.org/10.5167/uzh-137221>

Journal Article

Accepted Version

Originally published at:

Grabher, Patrick; Mohammadi, Siawoosh; David, Gergely; Freund, Patrick (2017). Neurodegeneration in the spinal ventral horn prior to motor impairment in cervical spondylotic myelopathy. *Journal of Neurotrauma*, 34(15):2329-2334.

DOI: <https://doi.org/10.1089/neu.2017.4980>

Neurodegeneration in the spinal ventral horn prior to motor impairment in cervical spondylotic myelopathy

Patrick Grabher¹, PhD, Siawoosh Mohammadi^{2,3,4}, PhD, Gergely David¹, MSc, Patrick Freund^{1,3,4,5}, MD PhD

¹ Spinal Cord Injury Center Balgrist, University Hospital Zurich, University of Zurich, Zurich, Switzerland

² Department of Systems Neuroscience, University Medical Center Hamburg-Eppendorf, Hamburg, Germany

³ Wellcome Trust Centre for Neuroimaging, Institute of Neurology, University College London, London, UK

⁴ Department of Neurophysics, Max Planck Institute for Human Cognitive and Brain Sciences, Leipzig, Germany

⁵ Department of Brain Repair and Rehabilitation, Institute of Neurology, University College London, London, UK

Running title: Grey matter degeneration in CSM

Table of Contents Title: Ventral and dorsal horn degeneration in cervical spondylotic myelopathy

Patrick Freund, MD PhD (Corresponding author)

Spinal Cord Injury Center, Balgrist University Hospital

Forchstrasse 340, 8008 Zürich, Switzerland

Telephone: +41 44 510 72 11

Fax: +41 44 386 39 09

E-Mail: patrick.freund@balgrist.ch

Patrick Grabher, PhD

Spinal Cord Injury Center, Balgrist University Hospital

Forchstrasse 340, 8008 Zürich, Switzerland

Telephone: +41 44 510 72 13

Fax: +41 44 386 39 09

E-Mail: patrick.grabher@balgrist.ch

Siawoosh Mohammadi, PhD

Department of Systems Neuroscience, University Medical Center Hamburg-Eppendorf

Martinistrasse 52, 20246 Hamburg, Germany

Telephone: +49 40 7410 54753

Fax: +41 44 386 39 09

E-Mail: s.mohammadi@uke.de

Gergely David, MSc

Spinal Cord Injury Center, Balgrist University Hospital

Forchstrasse 340, 8008 Zürich, Switzerland

Telephone: +41 44 510 72 13

Fax: +41 44 386 39 09

E-Mail: gergely.david@balgrist.ch

Abstract

Remote grey matter pathology has been suggested rostral to the compression site in cervical spondylotic myelopathy (CSM). We therefore assessed neurodegeneration in the grey matter ventral and dorsal horns.

Twenty patients with CSM and eighteen healthy subjects underwent a high-resolution structural and diffusion MRI protocol at vertebra C2/C3. Patients received comprehensive clinical assessments. T2*-weighted data provided cross-sectional area measurements of grey matter ventral and dorsal horns to identify atrophy. At the identical location, mean diffusivity (MD) and fractional anisotropy (FA) determined the microstructural integrity. Finally, the relationships between neurodegeneration occurring in the grey and white matter and clinical impairment were investigated.

Patients suffered from mild to moderate CSM with mainly sensory impairment. In the ventral horns, cross-sectional area was not reduced ($p=0.863$), but MD was increased ($p=0.045$). The magnitude of MD changes within the ventral horn was associated with white matter diffusivity changes (MD: $p=0.013$; FA: $p=0.028$) within the lateral corticospinal tract. In contrast, dorsal horn cross-sectional area was reduced by 16.0% ($p<0.001$) without alterations in diffusivity indices when compared to controls. No associations between the magnitude of ventral and dorsal horn neurodegeneration and clinical impairment were evident.

Focal cord grey matter pathology is evident remote to the compression site in-vivo in CSM patients. Microstructural changes in the ventral horns (i.e. motoneurons) related to corticospinal tract integrity in the absence of atrophy and marked motor impairment. Dorsal horn atrophy corresponded to main clinical representation of sensory impairment. Thus, neuroimaging biomarkers of cord grey matter integrity reveal focal neurodegeneration prior to marked clinical impairment and thus could serve as predictors of ensuing impairment in CSM patients.

Keywords: Spinal Cord Diseases, Myelopathy, Diffusion Tensor Imaging, Spinal Cord Dorsal Horn, Spinal Cord Ventral Horn

Introduction

Cervical spondylotic myelopathy (CSM) is the most frequent non-traumatic spinal cord disorder in the elderly leading to impairment in sensorimotor function and reduced quality of life.¹ In addition, it is a known risk factor for cervical central cord syndrome (i.e. spinal cord injury).² However, the onset of cord compression is unknown and the trajectory of disease progression remains often subclinical for years.

Damage to the neuronal tissue is progressively caused by chronic cord compression, exposure to dynamic stress, and deterioration of blood-supply.³ Next to focal myelopathy,^{4–6} a cascade of neurodegenerative processes is evident in the grey and white matter above the site of compression in the cervical cord^{7–10} and even in the sensorimotor cortex^{11,12} that can be assessed non-invasively, amongst others, by magnetic resonance spectroscopy and diffusion tensor imaging (DTI) and other advanced MRI techniques sensitive to atrophy and microstructural changes.¹³ Microstructural changes can be identified by diffusivity indices (e.g. fractional anisotropy (FA) and mean diffusivity (MD)) calculated by DTI that provide information about the microstructural integrity of the underlying tissue. Reduced FA and increased MD have both been associated with loss of axonal count and myelin content.^{14–16}

Neuroprotective treatments^{6,17} to improve functional independence and quality of life have entered clinical trials.¹⁸ However, there is a need to detect and monitor subclinical trajectories prior to marked clinical impairment in tissue at risk (i.e. before relevant irreversible neuronal loss) **that may improve interventional guidelines (e.g. decompressive surgery)**, to evaluate individual (subclinical) treatment responses and to predict outcome. Advanced neuroimaging biomarkers of cord pathology therefore hold promise to bridging this gap.¹⁹

In this study, we investigated detailed grey matter ventral and dorsal horn atrophy (i.e. volumetric reduction) and microstructural alterations (i.e. changes in diffusivity indices) using high-resolution structural and diffusion MRI protocols above stenosis in the cervical spinal cord in patients with CSM.⁷ This allows us to address key questions of whether both the ventral and dorsal horns show signs of neurodegeneration prior to onset of marked

impairment rostral to the site of compression and whether the extent of grey matter pathology relates to white matter pathology (e.g. relation between motor neurons and corticospinal tract).

Methods

Participants and study design

Twenty patients (six female, age 52.0 ± 14.5 years (mean \pm SD)) with CSM referred for neurological examination due to sensory impairment and pain and eighteen healthy subjects (six female, age 44.4 ± 9.7 years) were consecutively recruited in the outpatient clinic. Tract-specific white matter changes in the posterior column and corticospinal tracts were already reported for this study cohort.⁷ Age was statistically not different between patients and controls (Mann-Whitney U test: $p=0.1075$). Following inclusion criteria for study enrolment were fulfilled from all participants: age between 18-70 years, no MRI contradictions, no other neurological or mental conditions, and no pregnancy. The study protocols were in accordance with the Declaration of Helsinki and approved by the local review board (reference number: EK-2012-0343). All participants gave written informed consent before study inclusion.

Clinical examination

All patients underwent a comprehensive clinical protocol including the modified Japanese Orthopedic Association (mJOA) scale²⁰ to assess disease severity and sensorimotor function. The International Standards for Neurological Classification of Spinal Cord Injury (ISNCSCI) protocol²¹ for upper extremity motor score (UEMS), light touch (UELTL) and pinprick (UEPP), the Spinal Cord Independence Measure (SCIM),²² and the Graded Redefined Assessment of Strength, and Sensibility and Prehension (GRASSP)²³ were used as complementary assessments.

MRI data acquisition

In all participants, high-resolution MRI data at vertebra C2/C3 (above the level of compression in all patients) was acquired on a 3T Skyra^{fit} MRI scanner (Siemens Healthcare, Germany) equipped with a 16-channel radio-frequency receive head and neck coil. A MRI-compatible stiff neck (Laerdal Medicals, Norway) was worn by all participants to reduce motion artefacts in z direction. All participants were carefully positioned by the radiographers.

As reported previously⁷, the midsagittal slice of a 2D sagittal T2-weighted turbo spin-echo sequence of the cervical spine was used for assessing the site of compression, to calculate the maximum canal compromise (MCC) and the maximum spinal cord compression (MSCC). We further quantified the signal change ratio from the region of hyperintensity against an average reference region at the C7/T1 and C2 level or, if not applicable, from the level of greatest cord compression at C2. The scan specification were the following: 20 slices with a thickness of 2.5mm with 10% inter-slice gap, field of view (FOV) of 220x220mm², matrix size of 384x384, time of repetition (TR) of 3760ms, time of echo (TE) of 87ms, flip angle $\alpha=160^\circ$, readout bandwidth of 260Hz/pixel and a total acquisition time of 2 minutes and 2 seconds.

We used a high-resolution 3D T2*-weighted MEDIC (multi-echo data imaging combination) sequence to acquire five structural volumes with the following parameters: field of view (FOV)=162x192mm², matrix size=648x768, twenty slices perpendicular to the spinal cord, voxel size=0.25x0.25x2.50mm³, TR=44ms, TE=19ms, flip angle=11°, and readout bandwidth=260Hz/pixel.

We used a cardiac-gated monopolar single-shot spin-echo EPI (echo-planar imaging) sequence with reduced FOV and outer volume suppression^{24,25} to acquire four diffusion-weighted (DW) datasets including 30 DW volumes ($b=500\text{s/mm}^2$) and six T2-weighted volumes ($b=0\text{s/mm}^2$). In total, 144 DW volumes were acquired. Sequence parameters were as following: FOV=133x30mm², matrix size=176x40, ten slices perpendicular to spinal cord with 10% inter-slice gap, voxel size=0.8x0.8x5mm³, TR=350ms, TE=73ms, and readout bandwidth=768Hz/pixel.

Quantitative MRI data processing

We used SPM12 (<http://www.fil.ion.ucl.ac.uk/spm/>) to register the five 3D structural volumes to account for non-rigid motion and increase signal to noise using a symmetric diffeomorphic algorithm.²⁶ Jim 7.0 (Xynapse Systems, UK) was used to manually segment the cross-sectional spinal cord grey matter⁷ and further subdivision into the bilateral ventral (approximately Rexed lamina VI-IX) and dorsal (approximately Rexed lamina I-V) horns (Figure 1A). Lamina X was excluded due to high intra-rater variability. The coefficients of variation (COV=standard deviation/mean) for intra-rater variability of grey

matter, ventral horn, and dorsal horn areas was 2.8%, 3.6%, 5.6% (five healthy controls, three segmentations at least 2 weeks apart), and inter-rater variability of 5.5%, 12.3%, and 15.2% (all healthy controls, two independent raters), respectively.²⁷

For diffusion data, we used the ACID toolbox (www.diffusiontools.com) for eddy current, motion, and physiological artefacts correction^{28,29} and for robust tensor fitting²⁹. Mean diffusivity (MD) and fractional anisotropy (FA) were calculated and normalized to the MNI-Poly-AMU template³⁰ using the FA voxel-based statistics toolbox.³¹ Additionally, manual slice-by-slice registration refined the registration accuracy.⁷ Diffusion indices maps were smoothed with a $0.5 \times 0.5 \times 5 \text{ mm}^3$ full-width at half maximum Gaussian kernel.

MRI data analysis

Stata 13 (StataCorp LP, USA) was used to assess differences in cross-sectional areas of ventral and dorsal horns (i.e. atrophy) between groups using analysis of covariance (ANCOVA). Regression models were constructed to investigate the relationship between volumetric grey matter readouts and clinical impairment **and level of compression**.

SPM12 was used for voxel-wise statistics using general linear models in calculated diffusivity maps to assess microstructural alterations. Statistical parametric maps were initially thresholded with a cluster-defining threshold of $p=0.01$. A cluster extent threshold of $p=0.05$ based on Gaussian Random Field theory was applied to account for multiple comparisons³² and only results corrected for family-wise error are reported. Two-sample t-tests were used to assess differences in grey matter diffusivity indices between groups. Regression models were constructed to assess the relationship between grey matter and **1) corresponding white matter tract diffusivities, 2) level of compression, and 3) clinical impairment**. A grey matter atlas was used as region of interest in all voxel-wise statistical models of diffusivity indices.³⁰

Age was included as nuisance variable in all statistical models assessing atrophy and microstructural alterations to reduce age-dependent variance and adjust for possible confounding effects.

Results

In brief, cervical spondylotic myelopathy was identified as mild in ten patients (mJOA ≥ 15), as moderate in nine patients (mJOA = 12–14) and as severe in one patient (mJOA < 12). Nine from 20 patients showed a T2 signal hyperintensity with a signal change ratio of 1.58 ± 0.32 and the level of stenosis was at C3/4 for two patients, at C4/C5 for one patient, at C5/C6 for 13 patients, at C6/7 for three patients, and at C7/C8 for one patient. The maximum spinal cord compression (MSCC) was $17.33 \pm 7.21\%$ and maximum canal compromise (MCC) $37.36 \pm 8.58\%$. Complementary assessments of sensorimotor function (mean \pm SD) were as follows: upper-extremity light-touch (UELTL) = 27.70 ± 4.07 , pinprick (UEPP) = 27.30 ± 3.77 , and motor score (UEMS) = 49.70 ± 0.50 ; spinal cord independence measure (SCIM) = 97.85 ± 4.04 ; and graded redefined assessment of strength, sensibility and prehension (GRASSP) = 220.74 ± 12.32 . In patients, level of stenosis was at C3/4 (n=2), at C4/C5 (n=1), at C5/C6 (n=13), at C6/7 (n=3), and at C7/C8 (n=1). Eight patients showed a single compression site, whereas 12 patients showed a multisegmental degeneration of the spinal column. Detailed individual patients characteristics and radiologic readouts (i.e. maximum spinal cord compression, maximum canal compromise, and signal hyperintensities) were reported previously.⁷

We first confirmed the reductions in cross-sectional cervical spinal cord, white matter, and grey matter area in patients compared to controls.⁷ Grey matter area was reduced by 7.4% ($p=0.021$; patients: $14.98 \pm 1.46\text{mm}^2$ (mean \pm SD); controls $16.18 \pm 0.89\text{mm}^2$). In the bilateral ventral horns, the cross-sectional area was not different between groups ($p=0.863$; patients: $6.42 \pm 0.76\text{mm}^2$; controls: $6.46 \pm 0.44\text{mm}^2$) (Figure 1B), but MD was increased ($p=0.045$, $k=67\text{mm}^3$, $Z=3.22$, $x=-2.5\text{mm}$, $y=-19\text{mm}$, $z=36\text{mm}$) (Figure 2A&B). No significant between group changes were evident for FA. The cross-sectional area of bilateral dorsal horns was reduced by 16.0% in patients compared to controls ($p<0.001$; patients: $6.94 \pm 1.13\text{mm}^2$; controls $8.26 \pm 0.77\text{mm}^2$) (Figure 1B), but no significant diffusivity changes were detected.

Investigating the relationship between grey and white matter diffusivities, we observed an association between the increased right ventral horn MD and increased MD ($p=0.013$, $k=98\text{mm}^3$, $Z=5.25$, $x=3.5\text{mm}$, $y=-19.5\text{mm}$, $z=19\text{mm}$) and reduced FA ($p=0.028$, $k=74\text{mm}^3$,

Z=4.53, x=4.5mm, y=-18.5mm, z=30mm) in the corresponding right corticospinal tract (Figure 2A&C).

No associations were observed for any grey matter MRI readouts and **level of compression or clinical impairment**.

Discussion

In a cohort of CSM patients in which atrophy of grey and white matter was reported⁷, we now addressed to what extent the degree of neurodegeneration (i.e. atrophy and diffusivity changes) in the ventral and dorsal horns relates to white matter integrity changes of the major spinal pathways and clinical impairment. We show detailed grey matter neurodegeneration occurring in the ventral and dorsal horns of the cervical cord grey matter rostral to the site of compression in patients with mild to moderate CSM. Crucially, focal grey matter neurodegeneration in the ventral horns was related to a decreased integrity of the corticospinal tract prior to marked impairment in motor function.^{1,2}

Insights into spinal cord grey matter pathology

At the compression site, focal neurodegeneration is evident by grey matter atrophy in parallel to axonal degeneration of spinal pathways^{4,5} that are caused by compression-induced ischemia,^{17,33} neuroinflammation^{6,33,34} and neuronal loss.^{6,33}

In this study, we show extensive neurodegeneration several segments above the level of compression in the spinal ventral and dorsal horns in-vivo. Interestingly, the ventral horns showed diffusivity changes (i.e. increased MD) in the absence of atrophy. Propriospinal circuitries^{35,36} and corticospinal projections to motor neurons³⁷ might be indirectly perturbed by the stenosis leading to remote neurodegeneration (e.g. axonal degeneration, neuronal loss)^{3,38} which cause the mean diffusivity to increase. On the contrary, in the dorsal horns, prominent atrophy in the absence of diffusivity changes was evident above the compression site. Remote dorsal horn atrophy rostral to the injury site may be caused by anterograde and transsynaptic degeneration^{38–40} and triggered by focal damage to the ascending fibres of the spinothalamic tract and somatosensory afferents transmitting to second-order sensory pathways⁴¹. These findings are coherent with the clinical representation of predominantly sensory impairment and pain in this CSM patient cohort. Another factor of dorsal horn atrophy might be a result of loss of afferent control of the corticospinal tract.^{42,43} Thus, in the absence of ventral horn atrophy, dorsal horn atrophy

was the major factor contributing to grey matter volumetric degeneration above the compression site in this patient cohort.

Interestingly, the overall butterfly shape of the grey matter was not altered in any patient remote from stenosis. **In contrast, at the site of compression the grey and white matter was not readily distinguishable on the MEDIC sequence due to partial volume effects caused by the compression of the myelon. Thus, measuring above the site of compression overcomes these technical challenges enabling the accurate and sensitive sub-segmentation of white and grey matter as well as unbiased voxel-based analysis of microstructure. Moreover, measuring above the level of compression offers greater sensitivity to capturing overall neurodegeneration as compression occurs frequently at multiple levels and thus the full extent of neurodegeneration can only be captured above. This approach is widely applied in MS⁴⁴ and SCI⁴⁵ where a spinal injury can occur at any level of the cord. Thus assessing neurodegeneration above and potentially below the level of compression site holds promise to complement clinical readouts.**

In summary, neurodegeneration in CSM, although different in causation, disease onset and progression trajectory,³ resembles the pathophysiological processes of antero- and retrograde degeneration observed after spinal cord injury.^{38,46,47}

Relating grey matter pathology to white matter pathology and impairment

In CSM, neurodegeneration is evident far beyond the site of compression impacting both grey and white matter integrity.⁷⁻¹² We provide a link between focal grey matter changes (e.g. motor neuron damage) and remote white matter changes by revealing a direct relationship between right ventral horn diffusivity changes (i.e. MD increases) and white matter diffusivity changes along the corticospinal tract (i.e decreased FA). We observed similar findings on the contralateral left side, but they did not survive correction for multiple comparisons. Ventral horn and corticospinal diffusivity changes may therefore indicate early microstructural neurodegeneration of the motor system before onset of marked motor impairment. **No relationship was observed for remote grey matter neurodegeneration and level of compression. The complex nature of neurodegeneration**

and its dependence on a combination of multiple linear and/or non-linear factors (e.g. distance to compression, single vs. multiple spinal degeneration, treatments) may have concealed a linear relationship.

The current clinical outcome measures (e.g. mJOA) are dominated by focal cord compression and white matter pathology, but they are not sensitive to detect remote changes in the sensorimotor neuronal pool and interneuronal circuits located within the grey matter at the cervical C2/C3 level. In accordance to this, we observed no associations between grey matter MRI readouts above the site of compression and clinical scores. This study therefore motivates the development of novel and more refined readouts to complement clinical assessments.

Following considerations should be taken into account. Age was not significantly different, but still might have some effects on the MRI data. Therefore, we included age as covariate of no interest in all statistical models to reduce possible confounds. Grey matter segmentation and partition into ventral and dorsal horns was performed manually as fully automated frameworks are still in development.³⁰ Inter- and intra-observer coefficient of variation for grey matter segmentation are similar to the ones previously reported.²⁷ In addition, intra-observer variability in grey matter horns was below 6%. Voxel-based statistics in spinal cord imaging is still in its infancy and depends on acquisition and post-processing techniques to reduce artefacts due to instrumental (e.g. eddy currents) and physiological noise (e.g. cardiac pulsation), and subject motion. Therefore, we used state-of-the-art acquisition and post-processing techniques feasible in clinical settings to reduce these confounding effects. For our voxel-based statistical analysis within the cervical grey matter, we used a grey matter template³⁰ as region of interest to increase sensitivity.

Misalignment of grey matter during registration and normalization may reduce the sensitivity for true positive results by increasing the between subject variability. For example, in the dorsal horns expected diffusivity changes might be harder to detect due to a higher misalignment of the dorsal horn as compared to the ventral horn. Another reason for the lack of observed diffusivity changes could be due to partial volume effects (PVE) between grey and white matter that may have masked microstructural changes (i.e. alterations in diffusivity indices) in the dorsal horns due to marked atrophy (i.e. diffusivity changes in grey matter due to white matter displacement).

Conclusion

Microstructural changes in the ventral horns above the level of injury and their interplay with diffusivity changes in the corticospinal tract indicate neurodegeneration affecting the motor system prior to marked clinical impairment. Dorsal horn atrophy occurred in parallel to sensory impairment and pain. Therefore, grey matter neuroimaging biomarkers **beyond the focal cord compression have to be considered as these** may provide clinically relevant readouts sensitive to subclinical structural changes and thereby complement conventional clinical readouts. **Future longitudinal studies applying advanced spinal cord neuroimaging biomarkers will aim to improve our understanding of the pathophysiological processes and evaluation of prognostic factors, which holds potential to improve disease management.**

Acknowledgements

This work was supported by the Clinical Research Priority Program “Neuro-Rehab” of the University of Zurich and the International Foundation for Research in Paraplegia. SM was supported by the Marie Skłodowska-Curie Individual Fellowship MSCA-IF-2015 (EU Horizon 2020).

Author Disclosure Statement

No competing financial interests exist.

References

1. Moore, A.P., and Blumhardt, L.D. (1997). A prospective survey of the causes of non-traumatic spastic paraparesis and tetraparesis in 585 patients. *Spinal Cord* 35, 361–367.
2. van Middendorp, J.J., Pouw, M.H., Hayes, K.C., Williams, R., Chhabra, H.S., Putz, C., Veth, R.P.H., Geurts, a C.H., Aito, S., Kriz, J., McKinley, W., van Asbeck, F.W. a, Curt, A., Fehlings, M.G., Van de Meent, H., Hosman, a J.F., and Collaborators, E.-S.S.G. (2010). Diagnostic criteria of traumatic central cord syndrome. Part 2: a questionnaire survey among spine specialists. *Spinal cord Off. J. Int. Med. Soc. Paraplegia* 48, 657–663.
3. Karadimas, S.K., Gatzounis, G., and Fehlings, M.G. (2014). Pathobiology of cervical spondylotic myelopathy. *Eur. Spine J.* 24, 132–138.
4. Nakano, K.K., Schoene, W.C., Baker, R. a, and Dawson, D.M. (1978). The cervical myelopathy associated with rheumatoid arthritis: analysis of patients, with 2 postmortem cases. *Ann Neurol* 3, 144–151.
5. Ito, T., Oyanagi, K., Takahashi, H., Takahashi, H.E., and Ikuta, F. (1996). Cervical spondylotic myelopathy. Clinicopathologic study on the progression pattern and thin myelinated fibers of the lesions of seven patients examined during complete autopsy. *Spine (Phila. Pa. 1976)*. 21, 827–833.
6. Yu, W.R., Liu, T., Kiehl, T.-R., and Fehlings, M.G. (2011). Human neuropathological and animal model evidence supporting a role for Fas-mediated apoptosis and inflammation in cervical spondylotic myelopathy. *Brain* 134, 1277–1292.
7. Grabher, P., Mohammadi, S., Trachsler, A., Friedl, S., David, G., Sutter, R., Weiskopf, N., Thompson, A.J., Curt, A., and Freund, P. (2016). Voxel-based analysis of grey and white matter degeneration in cervical spondylotic myelopathy. *Sci. Rep.* 6, 24636.
8. Salamon, N., Ellingson, B.M., Nagarajan, R., Gebara, N., Thomas, A., and Holly, L.T. (2013). Proton magnetic resonance spectroscopy of human cervical spondylosis at 3T. *Spinal Cord* 51, 558–563.
9. Ellingson, B.M., Salamon, N., Hardy, A.J., and Holly, L.T. (2015). Prediction of neurological impairment in cervical spondylotic myelopathy using a combination of diffusion mri and proton mr spectroscopy. *PLoS One* 10, 1–14.
10. Martin, A.R., De Leener, B., Cohen-Adad, J., Aleksanderek, I., Cadotte, D.W., Kalsi-Ryan, S., Tetreault, L., Crawley, A., Ginsberg, H.J., and Fehlings, M.G. (2016). 163 Microstructural MRI Quantifies Tract-Specific Injury and Correlates With Global Disability and Focal Neurological

- Deficits in Degenerative Cervical Myelopathy. *Neurosurgery* 63, 165.
11. Goncalves, S., Stevens, T.K., Doyle-Pettypiece, P., Bartha, R., and Duggal, N. (2016). N-acetylaspartate in the motor and sensory cortices following functional recovery after surgery for cervical spondylotic myelopathy. *J. Neurosurg. Spine* 25, 1–8.
 12. Kowalczyk, I., Duggal, N., and Bartha, R. (2012). Proton magnetic resonance spectroscopy of the motor cortex in cervical myelopathy. *Brain* 135, 461–468.
 13. Martin, A.R., Aleksanderek, I., Cohen-Adad, J., Tarmohamed, Z., Tetreault, L., Smith, N., Cadotte, D.W., Crawley, A., Ginsberg, H., Mikulis, D.J., and Fehlings, M.G. (2016). Translating state-of-the-art spinal cord MRI techniques to clinical use: A systematic review of clinical studies utilizing DTI, MT, MWF, MRS, and fMRI. *NeuroImage Clin.* 10, 192–238.
 14. Cohen-Adad, J., El Mendili, M.M., Lehericy, S., Pradat, P.F., Blancho, S., Rossignol, S., and Benali, H. (2011). Demyelination and degeneration in the injured human spinal cord detected with diffusion and magnetization transfer MRI. *Neuroimage* 55, 1024–1033.
 15. Gouw, A.A., Seewann, A., Vrenken, H., van der Flier, W.M., Rozemuller, J.M., Barkhof, F., Scheltens, P., and Geurts, J.J. (2008). Heterogeneity of white matter hyperintensities in Alzheimer's disease: post-mortem quantitative MRI and neuropathology. *Brain* 131, 3286–3298.
 16. Schmierer, K., Wheeler-Kingshott, C. a M., Boulby, P. a, Scaravilli, F., Altmann, D.R., Barker, G.J., Tofts, P.S., and Miller, D.H. (2007). Diffusion tensor imaging of post mortem multiple sclerosis brain. *Neuroimage* 35, 467–477.
 17. Karadimas, S.K., Laliberte, A.M., Tetreault, L., Chung, Y.S., Arnold, P., Foltz, W.D., and Fehlings, M.G. (2015). Riluzole blocks perioperative ischemia-reperfusion injury and enhances postdecompression outcomes in cervical spondylotic myelopathy. *Sci. Transl. Med.* 7, 316ra194.
 18. Fehlings, M.G., Wilson, J.R., Karadimas, S.K., Arnold, P.M., and Kopjar, B. (2013). Clinical Evaluation of a Neuroprotective Drug in Patients With Cervical Spondylotic Myelopathy Undergoing Surgical Treatment. *Spine (Phila. Pa. 1976)*. 38, S68–S75.
 19. Weiskopf, N., Mohammadi, S., Lutti, A., and Callaghan, M.F. (2015). Advances in MRI-based computational neuroanatomy: from morphometry to in-vivo histology. *Curr. Opin. Neurol.* 28, 313–22.
 20. Benzel, E.C., Lancon, J., Kesterson, L., and Hadden, T. (1991). Cervical laminectomy and dentate ligament section for cervical spondylotic myelopathy. *J. Spinal Disord.* 4, 286–295.

21. Kirshblum, S.C., Waring, W., Biering-Sorensen, F., Burns, S.P., Johansen, M., Schmidt-Read, M., Donovan, W., Graves, D., Jha, A., Jones, L., Mulcahey, M.J., and Krassioukov, A. (2011). Reference for the 2011 revision of the International Standards for Neurological Classification of Spinal Cord Injury. *J. Spinal Cord Med.* 34, 547–554.
22. Itzkovich, M., Gelernter, I., Biering-Sorensen, F., Weeks, C., Laramée, M.T., Craven, B.C., Tonack, M., Hitzig, S.L., Glaser, E., Zeilig, G., Aito, S., Scivoletto, G., Mecci, M., Chadwick, R.J., El Masry, W.S., Osman, A., Glass, C. a, Silva, P., Soni, B.M., Gardner, B.P., Savic, G., Bergström, E.M., Bluvstein, V., Ronen, J., and Catz, A. (2007). The Spinal Cord Independence Measure (SCIM) version III: Reliability and validity in a multi-center international study. *Disabil. Rehabil.* 29, 1926–1933.
23. Kalsi-Ryan, S., Curt, A., Verrier, M.C., and Fehlings, M.G. (2012). Development of the Graded Redefined Assessment of Strength, Sensibility and Prehension (GRASSP): reviewing measurement specific to the upper limb in tetraplegia. *J. Neurosurg. Spine* 17, 65–76.
24. Heidemann, R.M., Feiweier, T., Anwender, A., Fasano, F., Pfeuffer, J., and Turner, R. (2009). High resolution single-shot diffusion-weighted imaging with a combination of zoomed EPI and parallel imaging., in: *Proceedings of the 17th Annual Meeting of ISMRM, Honolulu, USA*,. pp. 2736.
25. Morelli, J.N., Runge, V.M., Feiweier, T., Kirsch, J.E., Williams, K.W., and Attenberger, U.I. (2010). Evaluation of a modified Stejskal-Tanner diffusion encoding scheme, permitting a marked reduction in TE, in diffusion-weighted imaging of stroke patients at 3 T. *Invest. Radiol.* 45, 29–35.
26. Ashburner, J., and Ridgway, G.R. (2013). Symmetric diffeomorphic modeling of longitudinal structural MRI. *Front. Neurosci.* 6, 1–19.
27. Yiannakas, M.C., Kearney, H., Samson, R.S., Chard, D.T., Ciccarelli, O., Miller, D.H., and Wheeler-Kingshott, C.A. (2012). Feasibility of grey matter and white matter segmentation of the upper cervical cord in vivo: A pilot study with application to magnetisation transfer measurements. *Neuroimage* 63, 1054–1059.
28. Mohammadi, S., Möller, H.E., Kugel, H., Müller, D.K., and Deppe, M. (2010). Correcting eddy current and motion effects by affine whole-brain registrations: evaluation of three-dimensional distortions and comparison with slice-wise correction. *Magn. Reson. Med.* 64, 1047–1056.
29. Mohammadi, S., Freund, P., Feiweier, T., Curt, A., and Weiskopf, N. (2013). The impact of

- post-processing on spinal cord diffusion tensor imaging. *Neuroimage* 70, 377–85.
30. De Leener, B., Lévy, S., Dupont, S.M., Fonov, V.S., Stikov, N., Louis Collins, D., Callot, V., and Cohen-Adad, J. (2016). SCT: Spinal Cord Toolbox, an open-source software for processing spinal cord MRI data. *Neuroimage* .
 31. Mohammadi, S., Keller, S.S., Glauche, V., Kugel, H., Jansen, A., Hutton, C., Flöel, A., and Deppe, M. (2012). The Influence of Spatial Registration on Detection of Cerebral Asymmetries Using Voxel-Based Statistics of Fractional Anisotropy Images and TBSS. *PLoS One* 7, e36851.
 32. Friston, K.J., Worsley, K.J., Frackowiak, R.S., Mazziotta, J.C., and Evans, a C. (1994). Assessing the significance of focal activations using their spatial extent. *Hum. Brain Mapp.* 1, 210–20.
 33. Karadimas, S.K., Moon, E.S., Yu, W.-R., Satkunendrarajah, K., Kallitsis, J.K., Gatzounis, G., and Fehlings, M.G. (2013). A novel experimental model of cervical spondylotic myelopathy (CSM) to facilitate translational research. *Neurobiol. Dis.* 54, 43–58.
 34. Felix, M.-S., Popa, N., Djelloul, M., Boucraut, J., Gauthier, P., Bauer, S., and Matarazzo, V. a. (2012). Alteration of forebrain neurogenesis after cervical spinal cord injury in the adult rat. *Front. Neurosci.* 6, 45.
 35. Lemon, R.N., and Griffiths, J. (2005). Comparing the function of the corticospinal system in different species: Organizational differences for motor specialization? *Muscle and Nerve* 32, 261–279.
 36. Isa, T., Ohki, Y., Alstermark, B., Pettersson, L.-G., and Sasaki, S. (2007). Direct and Indirect Cortico-Motoneuronal Pathways and Control of Hand/Arm Movements. *Physiology* 22, 145–152.
 37. Lemon, R.N. (2008). Descending Pathways in Motor Control. *Annu. Rev. Neurosci.* 31, 195–218.
 38. Buss, A., Brook, G. a, Kakulas, B., Martin, D., Franzen, R., Schoenen, J., Noth, J., and Schmitt, a B. (2004). Gradual loss of myelin and formation of an astrocytic scar during Wallerian degeneration in the human spinal cord. *Brain* 127, 34–44.
 39. Woods, T.M., Cusick, C.G., Pons, T.P., Taub, E., and Jones, E.G. (1999). Progressive transneuronal changes in the brainstem and thalamus after long-term dorsal rhizotomies in adult macaque monkeys. *J. Neurosci.* 20, 3884–3899.
 40. Darian-Smith, C., Hopkins, S., and Ralston, H.J. (2010). Changes in synaptic populations in

the spinal dorsal horn following a dorsal rhizotomy in the monkey. *J. Comp. Neurol.* 518, 103–117.

41. Reed, J.L., Liao, C., Qi, H., and Kaas, J.H. (2016). Plasticity and Recovery After Dorsal Column Spinal Cord Injury in Nonhuman Primates. *J. Exp. Neurosci.* 10, 11–21.
42. Rojas-Piloni, G., Martínez-Lorenzana, G., Condés-Lara, M., and Rodríguez-Jiménez, J. (2010). Direct sensorimotor corticospinal modulation of dorsal horn neuronal C-fiber responses in the rat. *Brain Res.* 1351, 104–114.
43. Wu, Y.-P., and Ling, E.-A. (1998). Transsynaptic changes of neurons and associated microglial reaction in the spinal cord of rats following middle cerebral artery occlusion. *Neurosci. Lett.* 256, 41–44.
44. Lycklama, G., Thompson, A., Filippi, M., Miller, D., Polman, C., Fazekas, F., and Barkhof, F. (2003). Spinal-cord MRI in multiple sclerosis. *Lancet Neurol.* 2, 555–562.
45. Huber, E., Curt, A., and Freund, P. (2015). Tracking trauma-induced structural and functional changes above the level of spinal cord injury. *Curr. Opin. Neurol.* 28, 365–72.
46. Grabher, P., Callaghan, M.F., Ashburner, J., Weiskopf, N., Thompson, A.J., Curt, A., and Freund, P. (2015). Tracking sensory system atrophy and outcome prediction in spinal cord injury. *Ann. Neurol.* 78, 751–761.
47. Freund, P., Weiskopf, N., Ashburner, J., Wolf, K., Sutter, R., Altmann, D.R., Friston, K., Thompson, A., and Curt, A. (2013). MRI investigation of the sensorimotor cortex and the corticospinal tract after acute spinal cord injury: a prospective longitudinal study. *Lancet Neurol.* 12, 873–881.

Figures Legend

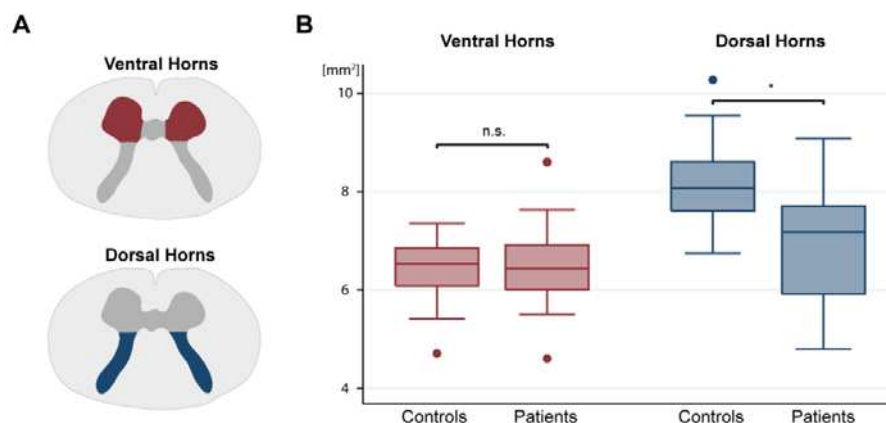


Figure 1: Cervical cord grey matter atrophy. (A) Illustration of grey matter sub-segmentation into dorsal (blue) and ventral (red) horns. (B) Significant reduction in cross-sectional area of dorsal horns, but not ventral horns in patients compared to healthy controls.

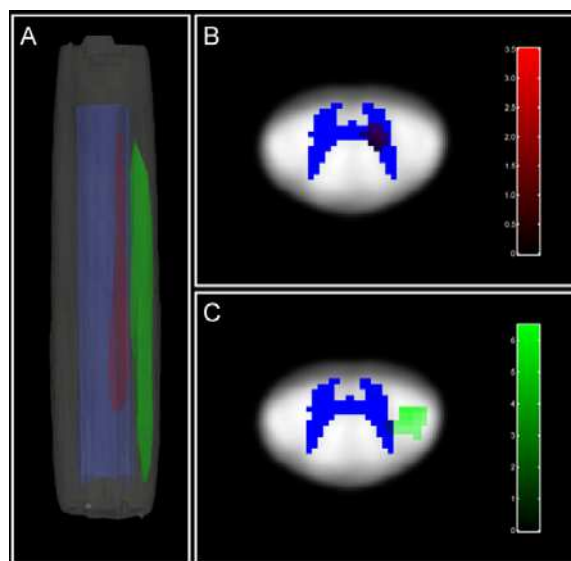


Figure 2: Microstructural changes in right ventral horn and corresponding right corticospinal tract. (A) Coronal section showing the extent of right ventral horn neurodegeneration (red) and its association with the right corticospinal tract (green). For reference, grey matter is shown in blue. **(B)** Axial section of elevated mean diffusivity in the right ventral horn (red) in patients compared to healthy controls. **(C)** Axial section showing the relationship between extracted mean diffusivity from the right ventral horn cluster shown in (B) and reduction of fractional anisotropy in the right corticospinal tract (green). Colour bars represent t-values. All results are FWE-corrected ($p < 0.05$).